

## Explaining LSND by a decaying sterile neutrino

Sergio Palomares-Ruiz,<sup>1,\*</sup> Silvia Pascoli,<sup>2,†</sup> and Thomas Schwetz<sup>3,‡</sup>

<sup>1</sup>*Department of Physics and Astronomy,  
Vanderbilt University, Nashville, TN 37235, USA*

<sup>2</sup>*Physics Department, Theory Division,  
CERN, CH-1211 Geneva 23, Switzerland*

<sup>3</sup>*Scuola Internazionale Superiore di Studi Avanzati,  
Via Beirut 2-4, I-34014 Trieste, Italy*

### Abstract

We propose an explanation of the LSND evidence for electron antineutrino appearance based on neutrino decay. We introduce a heavy neutrino, which is produced in pion and muon decays because of a small mixing with muon neutrinos, and then decays into a scalar particle and a light neutrino, predominantly of the electron type. We require values of  $gm_4 \sim \text{few eV}$ ,  $g$  being the neutrino–scalar coupling and  $m_4$  the heavy neutrino mass, e.g.  $m_4$  in the range from 1 keV to 1 MeV and  $g \sim 10^{-6}$ – $10^{-3}$ . Performing a fit to the LSND data as well as all relevant null-result experiments, we show that all data can be explained within this decay scenario. In the minimal version of the decay model, we predict a signal in the upcoming MiniBooNE experiment corresponding to a transition probability of the same order as seen in LSND. In addition, we show that extending our model to two nearly degenerate heavy neutrinos it is possible to introduce CP violation in the decay, which can lead to a suppression of the signal in MiniBooNE running in the neutrino mode. We briefly discuss signals in future neutrino oscillation experiments, we show that our scenario is compatible with bounds from laboratory experiments, and we comment on implications in astrophysics and cosmology.

---

\*Electronic address: sergio.palomares-ruiz@vanderbilt.edu

†Electronic address: Silvia.Pascoli@cern.ch

‡Electronic address: schwetz@sissa.it

## I. INTRODUCTION

The LSND experiment at LANSCE in Los Alamos took data from 1993–1998 and observed an excess of  $\bar{\nu}_e$  [1]. This was interpreted as evidence of  $\bar{\nu}_\mu \rightarrow \bar{\nu}_e$  transitions. The KARMEN experiment at the spallation source ISIS in England was looking at the same appearance channel in the years 1997–2001 at a slightly different baseline than LSND, but no positive signal was found [2]. Reconciling the evidence for  $\bar{\nu}_\mu \rightarrow \bar{\nu}_e$  appearance observed in LSND with the other evidence for neutrino oscillations [3, 4, 5, 6, 7] remains a challenge for neutrino phenomenology. It turns out that introducing a fourth sterile neutrino [8] does not lead to a satisfactory description of all data in terms of neutrino oscillations [9, 10] (see Ref. [11] for a recent update) because of tight constraints from atmospheric [3], solar [6], and null-result short-baseline (SBL) experiments [2, 12, 13, 14]. In view of this, several alternative explanations have been proposed, some of them involving very speculative physics: four-neutrino oscillations plus neutrino decay [15], three neutrinos and CPT violation [10, 16], a lepton number violating muon decay [17], five-neutrino oscillations [18], four neutrinos and CPT violation [19], a low-reheating-temperature Universe [20], CPT-violating quantum decoherence [21], mass-varying neutrinos [22], and shortcuts of sterile neutrinos in extra dimensions [23]. A critical test of the LSND signal will come soon from the MiniBooNE experiment [24], which is looking for  $\nu_\mu \rightarrow \nu_e$  appearance in a similar range of  $L/E_\nu$  as LSND,  $L$  being the distance travelled by the neutrinos and  $E_\nu$  their energy.

In this work we assume the existence of heavy (mainly sterile) neutrinos,  $n_h$ , with a small mixing with the muon neutrino. We denote their masses by  $m_h$ . The LSND signal is explained through the decay of  $n_h$  into a light neutrino, mixed predominantly with the electron neutrino. A natural way to introduce neutrino decays is by means of a term in the Lagrangian, which couples neutrinos to a light scalar, similar to the so-called Majoron models [25]. This term can be related to the neutrino mass generation mechanism through the spontaneous breaking of a lepton number symmetry via a non-zero vacuum expectation value of the scalar field. Similarly to these models, we introduce an interaction term between  $n_h$ , light neutrinos and a scalar. However, as we are only interested in the phenomenological consequences of such a term for the LSND experiment as well as for the other relevant neutrino experiments, we assume that this term arises at low energy as an effective interaction, not necessarily related to neutrino mass generation. We show that in the simplest case of one heavy sterile neutrino,  $n_4$ , for  $gm_4 \sim 1\text{--}10$  eV, e.g. neutrino masses around 100 keV and neutrino–scalar couplings  $g \sim 10^{-5}$ , LSND data can be explained in complete agreement with the null-results of other SBL neutrino experiments.

Light neutrino decay has been considered as an alternative solution to neutrino oscillations, to explain the atmospheric neutrino anomaly [26, 27] and the solar neutrino puzzle [26, 28]. Although the recent observation of an oscillatory behaviour in atmospheric neutrino [4] and KamLAND [7] data excludes a pure decay scenario as the possible explanation of these problems, a combined scenario of neutrino oscillations and decay is not excluded yet. We do not consider these possibilities here and we assume that atmospheric, solar and KamLAND neutrino transitions are explained by neutrino oscillations.

The decay of an exotic neutral massive particle, called karmino, produced in pion decays

was considered as a possible explanation for an anomaly seen in the first data set of the KARMEN experiment [29], which however, was not subsequently confirmed [30]. This hypothetical particle would move non-relativistically ( $\beta \sim 0.02$ ) from the source to the detector. If it were a massive neutrino, strong bounds on the mixing and lifetime could be placed from anomalous pion and muon decays [31] (for a recent review of the bounds, see Ref. [32]). Differently from this case, where no specific decay scenario was adopted, we assume here a Majoron-like type of decay. Furthermore, for typical values of masses, the heavy neutrino is relativistic at the energies in the LSND and KARMEN experiments, and we require it to decay before reaching the detector, with a lifetime much smaller than the one of the karmino.

An explanation of the LSND result invoking the interplay between neutrino oscillations and neutrino decay has been considered previously in Ref. [15]. A fourth neutrino is introduced with a mass of a few eV, which decays into a massless Goldstone boson (the Majoron) and into light neutrinos. The signal in LSND is provided by mixing, similar to (3+1) four-neutrino oscillations, whereas the decay serves to circumvent the constraints from the CDHS experiment. This approach requires very large couplings  $g \sim \mathcal{O}(10^3)$  and a mixing of  $\nu_e$  with the heavy mass state, and hence it appears to be in conflict with various bounds on neutrino–scalar couplings (see Section VII for a discussion). In contrast, in our model, the signal in the LSND experiment is provided entirely by the decay, and no mixing of  $\nu_e$  with the heavy neutrino is required. This allows us to invoke neutrino masses in the 100 keV range, which in turn permits a small coupling of  $g \sim 10^{-5}$ , in agreement with existing bounds.

The outline of the paper is as follows. In Section II we present the minimal decay framework and deduce the probabilities, which are needed to calculate the event rates. In Section III we present our analysis of LSND and KARMEN data within this scenario, and in Section IV we show that the decay framework is not in contradiction with any other null-result experiment by performing a combined analysis; we compare the quality of the fit to the one for oscillations. In Section V we discuss the prediction for MiniBooNE and other future neutrino experiments within the minimal decay framework, whereas in Section VI we show that, allowing for, at least, two sterile neutrinos and complex couplings, it is possible to obtain a CP-violating interference between oscillation and decay amplitudes, which would suppress the neutrino signal in MiniBooNE, but at the same time provide the antineutrino signal in LSND. In Section VII, we argue that our model is consistent with existing bounds from laboratory experiments, and we comment on implications for cosmology and astrophysics. In Section VIII we present our final remarks.

## II. DECAY FRAMEWORK AND TRANSITION PROBABILITIES

Let us consider the general case of  $N$  Majorana neutrinos. We take the three light neutrinos responsible for solar and atmospheric oscillations to be  $\nu_{1,2,3}$  with masses  $m_{1,2,3} \lesssim 1$  eV, while the heavy neutrinos have masses  $m_{4,5,\dots} \gg m_{1,2,3}$ . Furthermore we assume for the scalar mass  $m_{1,2,3} \lesssim m_\phi \ll m_{4,5,\dots}$ , such that the three light neutrinos are stable. Hence

the terms in the Lagrangian relevant to the decay (with scalar couplings<sup>1</sup>) are given, in the mass basis, by

$$\mathcal{L} = - \sum_{l,h} g_{hl} \bar{\nu}_{lL} n_{hR} \phi + \text{h.c.}, \quad (2.1)$$

where here and in the following the ranges for the indexes are  $l = 1, 2, 3$  and  $h = 4, 5, \dots$ . In general the coupling matrix  $g_{hl}$  will be complex.

In the case of Majorana particles, neutrinos are identical to antineutrinos. Weak interactions couple to left-handed (chiral) neutrinos and right-handed (chiral) antineutrinos while the propagation states are those of definite helicity. In the relativistic case, where helicity and chirality are approximately the same, one can identify neutrinos and antineutrinos with helicity states up to terms of order  $m/E_\nu$ . It follows from Eq. (2.1) that not only the decay  $n \rightarrow \bar{\nu} + \phi$  can occur, but also  $n \rightarrow \nu + \phi$  is possible [34]. Both processes are suppressed by terms of order  $m_h/E_{n_h}$ . For the former process the suppression is due to angular momentum conservation, while for the latter the chirality-flipping nature of the interaction, Eq. (2.1), is responsible for the suppression.<sup>2</sup>

In the approximation  $m_l \approx 0$ ,  $m_\phi \approx 0$  and  $m_h \ll E_{n_h}$ , the differential decay rate of an  $n_h$  of helicity  $r$  with energy  $E_{n_h}$  into a  $\nu_l$  of helicity  $s$  with energy  $E_{\nu_l}$  is

$$\frac{d\Gamma_{n_h^r \rightarrow \nu_l^s}(E_{n_h})}{dE_{\nu_l}} = \frac{1}{16\pi E_{n_h}^2} |\mathcal{M}_{rs}|^2, \quad (2.2)$$

where the indices  $r, s$  take the values ‘-’ for neutrinos and ‘+’ for antineutrinos, and the matrix element is given by<sup>3</sup>

$$|\mathcal{M}_{rs}|^2 = |g_{hl}|^2 m_h^2 \times \begin{cases} E_{\nu_l}/E_{n_h} & r = s \\ (1 - E_{\nu_l}/E_{n_h}) & r \neq s \end{cases}. \quad (2.3)$$

For relativistic neutrinos, the limiting values of the final neutrino energy are  $0 < E_{\nu_l} < E_{n_h}$ , and hence, the partial decay rate for  $n_h^r \rightarrow \nu_l^s + \phi$  for *both* cases, helicity-flipping ( $r \neq s$ ) and helicity-conserving ( $r = s$ ), is the same and given by [34]

$$\Gamma_{hl} = \Gamma_{n_h^r \rightarrow \nu_l^s} = \frac{|g_{hl}|^2 m_h^2}{32\pi E_{n_h}}. \quad (2.4)$$

The total decay rate of  $n_h$  is then given by  $\Gamma_h = 2 \sum_l \Gamma_{hl}$ .

<sup>1</sup> The case of pseudo-scalar couplings gives exactly the same results in the relativistic approximation we will use. It can also be shown that for processes in which all of the involved states are on-shell, a derivative interaction term can be rewritten in pseudo-scalar form [33].

<sup>2</sup> Throughout this work we will assume Majorana neutrinos. Here we just remark that in the case of Dirac neutrinos the decay is analogous. However, the decay products of the helicity-flipping channel are unobservable, since they are the right-(left-)handed component of the neutrino (antineutrino) fields, which do not participate in weak interactions.

<sup>3</sup> According to angular momentum conservation the matrix element Eq. (2.3) can be written also as  $|\mathcal{M}_{rs}|^2 = |g_{hl}|^2 m_h^2 (1 \mp \cos\theta)/2$  for  $r = s$  ( $r \neq s$ ), where  $\theta$  is the angle between the spin of  $n_h$  and the direction of  $\nu_l$  in the rest frame of  $n_h$ .

The flavour neutrinos  $\nu_\alpha$  ( $\alpha = e, \mu, \tau, s_1, s_2, \dots$ ) are related to the massive neutrinos in Eq. (2.1) by

$$\nu_\alpha = \sum_l U_{\alpha l} \nu_l + \sum_h U_{\alpha h} n_h. \quad (2.5)$$

The differential probability that an (anti)neutrino of flavour  $\alpha$  with energy  $E_{\nu_\alpha}$  is converted into an (anti)neutrino of flavour  $\beta$  with energy in the interval  $[E_{\nu_\beta}, E_{\nu_\beta} + dE_{\nu_\beta}]$  is:

$$\begin{aligned} \frac{dP_{\nu_\alpha^r \rightarrow \nu_\beta^s}(E_{\nu_\alpha})}{dE_{\nu_\beta}} &= \left| \sum_l U_{\beta l}^{(s)} U_{\alpha l}^{(r)*} \exp\left(-i\frac{m_l^2 L}{2E_{\nu_\alpha}}\right) \right|^2 \delta(E_{\nu_\alpha} - E_{\nu_\beta}) \delta_{rs} \\ &+ \left| \sum_h U_{\beta h}^{(s)} U_{\alpha h}^{(r)*} \exp\left(-i\frac{m_h^2 L}{2E_{\nu_\alpha}}\right) \exp\left(-\frac{\Gamma_h L}{2}\right) \right|^2 \delta(E_{\nu_\alpha} - E_{\nu_\beta}) \delta_{rs} \\ &+ W_{rs}(E_{\nu_\alpha}, E_{\nu_\beta}) \int_0^L dL' \frac{dP_{\nu_\alpha^r \rightarrow \nu_\beta^s}^{\text{dec}}}{dL'}, \end{aligned} \quad (2.6)$$

where we have introduced the notation  $X^{(r)} \equiv X$  for  $r = -$  and  $X^{(r)} \equiv X^*$  for  $r = +$ . In Eq. (2.6), we have used the fact that the light neutrinos  $\nu_l$  are not coherent with  $n_h$  because of the large mass difference, while both  $\nu_l$  and  $n_h$  are assumed to be coherent among themselves. The first term describes the oscillations of light neutrinos, whereas the second one describes oscillations of the heavy neutrinos weighted by the probability that they do not decay. These oscillation terms are only present in the helicity-conserving channel ( $r = s$ ). The third term describes the appearance of decay products, and is present for the helicity-conserving as well as helicity-flipping channels. Here  $W_{rs}(E_{\nu_\alpha}, E_{\nu_\beta})$  is the normalised energy distribution of the decay products:

$$W_{rs}(E_{\nu_\alpha}, E_{\nu_\beta}) \equiv \frac{1}{\Gamma_{hl}} \frac{d\Gamma_{n_h^r \rightarrow \nu_l^s}(E_{\nu_\alpha})}{dE_{\nu_\beta}} = 2 \Theta(E_{\nu_\alpha} - E_{\nu_\beta}) \times \begin{cases} E_{\nu_\beta}/E_{\nu_\alpha}^2 & r = s, \\ (E_{\nu_\alpha} - E_{\nu_\beta})/E_{\nu_\alpha}^2 & r \neq s, \end{cases} \quad (2.7)$$

where  $\Gamma_{hl}$  is the partial decay rate for  $n_h \rightarrow \nu_l$  given in Eq. (2.4). The relativistic approximation  $m_l \approx 0$  allows us to factor out  $W_{rs}(E_{\nu_\alpha}, E_{\nu_\beta})$  in Eq. (2.6). The term  $dP_{\nu_\alpha^r \rightarrow \nu_\beta^s}^{\text{dec}}/dL$  is the differential probability that the heavy component of the neutrino  $\nu_\alpha^r$  decays at the distance  $[L, L + dL]$  and the decay product interacts as a  $\nu_\beta^s$ . Adopting the effective operator method of Ref. [35] it can be calculated as

$$\frac{dP_{\nu_\alpha^r \rightarrow \nu_\beta^s}^{\text{dec}}}{dL} = \left| \sum_l U_{\beta l}^{(s)} \sum_h U_{\alpha h}^{(r)*} \mathcal{A}_{hl}^{(r)} \exp\left(-i\frac{m_h^2 L}{2E_{\nu_\alpha}}\right) \exp\left(-\frac{\Gamma_h L}{2}\right) \right|^2. \quad (2.8)$$

Here  $\mathcal{A}_{hl}$  is an effective amplitude for the decay of  $n_h$  into  $\nu_l$ , similar to the ‘‘appearance operator’’ of Ref. [35], and it is given by

$$\mathcal{A}_{hl} = g_{hl} A_h, \quad A_h \equiv \frac{\sqrt{\Gamma_{hl}}}{|g_{hl}|}. \quad (2.9)$$

Note that in the limit where the light neutrino masses can be neglected in the decay kinematics, the real quantity  $A_h$  is independent of the index  $l$ . Since for SBL experiments we

have  $\Delta m_{ll'}^2 L/E \ll 1$  we can neglect oscillations of the decay products to derive Eq. (2.8), but we include the possibility of oscillations of the heavy states before they decay.

In the simplest case in which  $N = 4$ , Eq. (2.8) becomes

$$\frac{dP_{\nu_\alpha^r \rightarrow \nu_\beta^s}^{\text{dec}}}{dL} = |U_{\alpha 4}|^2 |g_\beta^{rs}|^2 A_4^2 e^{-\Gamma_4 L}, \quad (2.10)$$

where we have defined the couplings in the flavour basis by

$$g_\beta^{rs} \equiv \sum_l U_{\beta l}^{(s)} g_{4l}^{(r)}. \quad (2.11)$$

### III. LSND AND KARMEN

Let us now calculate the  $\nu_\mu^r \rightarrow \nu_e^s$  appearance probability relevant to the LSND and KARMEN experiments. Unlike other explanations of the LSND result based on sterile neutrinos, our model does not require a mixing of the electron neutrino with the heavy mass state. Therefore, for simplicity we assume  $U_{e4} = 0$ . This implies that the first two lines in Eq. (2.6) disappear and using Eq. (2.10) we find

$$\frac{dP_{\nu_\mu^r \rightarrow \nu_e^s}(E_{\nu_\mu})}{dE_{\nu_e}} = W_{rs}(E_{\nu_\mu}, E_{\nu_e}) \frac{1}{2} |U_{\mu 4}|^2 R_e (1 - e^{-\Gamma_4 L}), \quad (3.1)$$

where we have defined the branching ratios by

$$R_\alpha \equiv \frac{|g_\alpha|^2}{\bar{g}^2}, \quad \bar{g}^2 \equiv \sum_l |g_{4l}|^2 = \sum_{\alpha=e,\mu,\tau,s} |g_\alpha|^2. \quad (3.2)$$

We have used  $\Gamma_4 = 2\bar{g}^2 A_4^2$ , and for simplicity we neglect the dependence of  $g_\alpha$  on the helicity indices, i.e. we neglect complex phases of  $U_{\alpha l}$  and  $g_{4l}$  (compare to Eq. (2.11)). The factor 1/2 in Eq. (3.1) accounts for the fact that half of the initial neutrinos decay into neutrinos and half of them into antineutrinos.

In LSND, neutrinos are produced by the decay at rest (DAR) of pions  $\pi^+ \rightarrow \mu^+ + \nu_\mu$  and by the subsequent decay of the muons  $\mu^+ \rightarrow e^+ + \nu_e + \bar{\nu}_\mu$ . In the detector, the appearance of  $\bar{\nu}_e$  is searched for by using the reaction  $\bar{\nu}_e + p \rightarrow e^+ + n$ . In case of oscillations, only the  $\bar{\nu}_\mu$  from the muon decay contribute to the signal. In the decay scenario, in addition, the  $\nu_\mu$  from the primary pion decay will give a contribution to the  $\bar{\nu}_e$  signal as well. Note that the  $\nu_e$  from the muon decay will not contribute to the signal because of our assumption  $U_{e4} = 0$ . The pion decay leads to a mono-energetic  $\nu_\mu$  beam with an energy of  $E_{\nu_\mu}^{(\pi)} = 29.8$  MeV, whereas the muon decay gives  $\bar{\nu}_\mu$  with a continuous spectrum,  $\phi_\mu(E_{\bar{\nu}_\mu})$ , rising up to  $E_{\bar{\nu}_\mu}^{\text{max}} = 52.8$  MeV. The total number of neutrinos is in both cases  $\phi_0 = \int dE_{\bar{\nu}_\mu} \phi_\mu(E_{\bar{\nu}_\mu})$ . The expected number of  $\bar{\nu}_e$  events with neutrino energy in the interval  $[E_{\bar{\nu}_e}, E_{\bar{\nu}_e} + dE_{\bar{\nu}_e}]$  is given by

$$\frac{dN}{dE_{\bar{\nu}_e}} = C \sigma(E_{\bar{\nu}_e}) \left[ \phi_0 \frac{dP_{\nu_\mu \rightarrow \bar{\nu}_e}(E_{\nu_\mu}^{(\pi)})}{dE_{\bar{\nu}_e}} + \int_{E_{\bar{\nu}_e}}^{E_{\bar{\nu}_\mu}^{\text{max}}} dE_{\bar{\nu}_\mu} \phi_\mu(E_{\bar{\nu}_\mu}) \frac{dP_{\bar{\nu}_\mu \rightarrow \bar{\nu}_e}(E_{\bar{\nu}_\mu})}{dE_{\bar{\nu}_e}} \right], \quad (3.3)$$

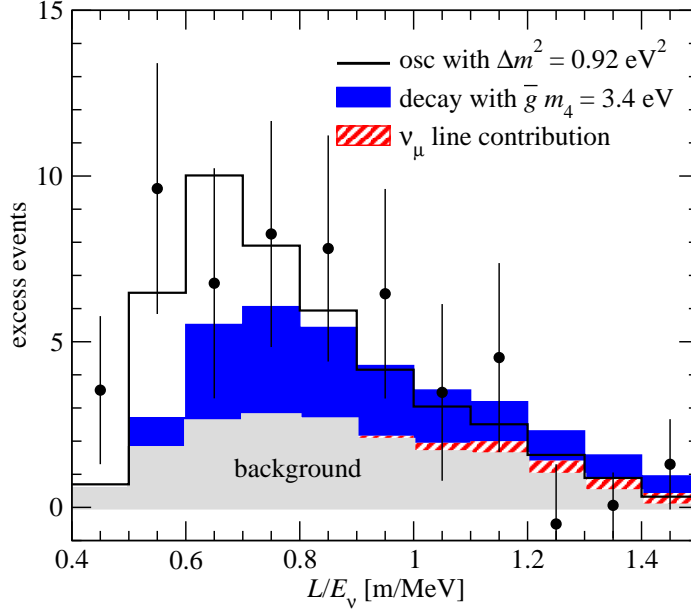


**FIG. 1:**  $L/E_\nu$  spectrum for LSND for decay and oscillations compared with the data given in Fig. 24 of Ref. [1]. The hatched histogram shows the contribution of the  $\nu_\mu$  line from the primary pion decay in the decay scenario.

where  $\sigma(E_{\bar{\nu}_e})$  is the detection cross section and  $C$  is an overall constant containing the number of target particles, efficiencies and geometrical factors. To calculate the observed number of events, we fold Eq. (3.3) with the energy resolution of the detector and integrate over the relevant energy interval.

For the statistical analysis of LSND data we use the total number of signal events implied by the transition probability  $P = (0.264 \pm 0.040)\%$  [1]. We have chosen an error such that we can reproduce Fig. 6 of Ref. [36], which is based on an event-by-event analysis of the DAR data. Furthermore we include spectral data in the form of 11 data points given in Fig. 24 of Ref. [1], where the beam excess is shown as a function of  $L/E_\nu$ . We fit these data with a free normalisation in order to avoid a double counting of the information given already by the total number of events. In our analysis we do not use the data from decay in flight (DIF) neutrinos, since the appearance signal in these data is less significant than in the DAR sample. Moreover, since the total number of DIF neutrinos is at most two orders of magnitude less than the  $\bar{\nu}_\mu$  flux from DAR, one does not expect a relevant contribution to the  $\bar{\nu}_e$  appearance signal from DIF due to the helicity-flipping decay.

Our analysis of LSND data gives a best fit value of  $\chi^2_{\min} = 5.6/9$  dof for oscillations and  $\chi^2_{\min} = 10.8/9$  dof for decay. The reason for the slightly worse fit for decay is the spectral distortion implied by the energy distribution of the decay products given in Eq. (2.7). In Fig. 1 we compare the best fit spectra for oscillations and decay with the data. In the decay scenario we predict slightly too many events at low energies and too few events in the high energy part of the spectrum. Note that the contribution of the  $\nu_\mu$  line from the primary pion decay is rather small. This follows from the fact that in the helicity-flipping decay mode, most of the decay products have a very small energy (see Eq. (2.7)), which implies that they

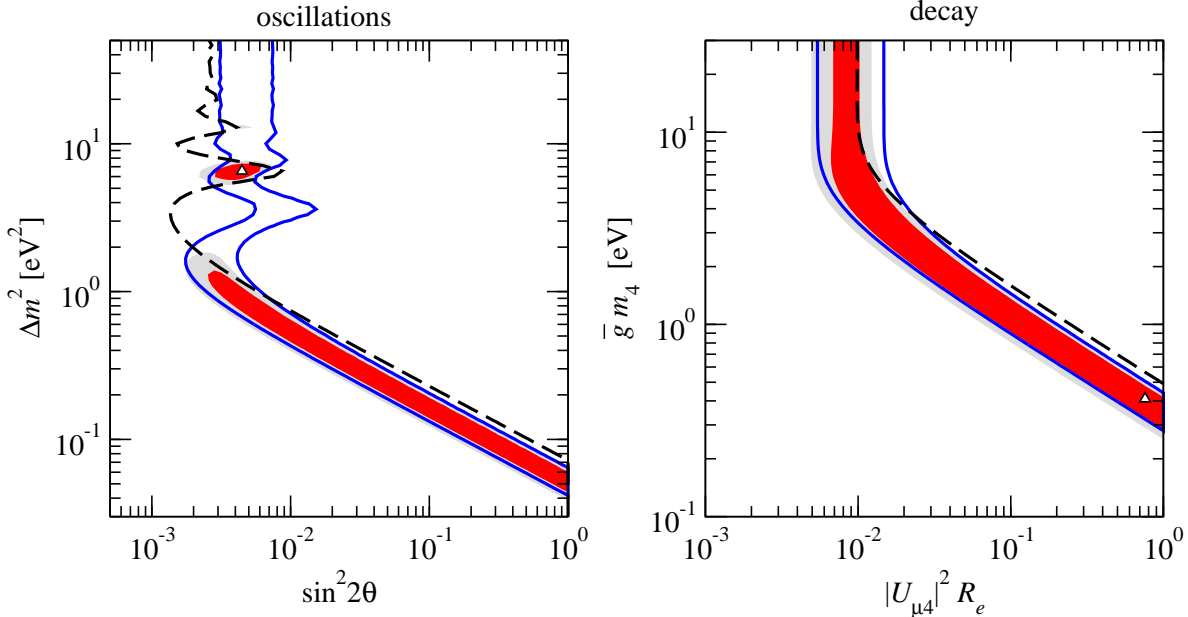


**FIG. 2:** Allowed regions for LSND (solid) and KARMEN (dashed) at 99% CL, and LSND and KARMEN combined (shaded regions) at 90% and 99% CL. The left panel corresponds to neutrino oscillations and the right panel to the decay scenario presented in this work.

fall below the detection threshold.<sup>4</sup> Although the fit in the decay scenario is slightly worse than for oscillations, the overall goodness of fit (GOF) is still acceptable. The  $\chi^2$  value cited above implies a GOF of 29%. Note, however, that a more refined analysis of the LSND spectral data might allow a significant discrimination between oscillations and decay. In the following we will assume that LSND data can be explained by our decay model and we shall proceed with the combination with other SBL data.

First we discuss the compatibility of LSND and KARMEN in the decay scenario (see Ref. [36] for a detailed analysis in the case of oscillations). Much as in LSND, also in KARMEN neutrinos are produced by the decay of pions at rest and the subsequent muon decay. However, in KARMEN detailed time information is available from the pulse structure of the proton beam and the excellent time resolution of the detector. Taking into account the muon lifetime of  $2.2 \mu\text{s}$  compared with the pion lifetime of 26 ns, a possible contribution of neutrinos from the pion decay was suppressed in the  $\bar{\nu}_\mu \rightarrow \bar{\nu}_e$  oscillation analysis by an appropriate time cut. Hence, in contrast to LSND the helicity-flipping decay of neutrinos from the  $\nu_\mu$  line does not contribute to the  $\bar{\nu}_e$  signal in KARMEN, and the first term in Eq. (3.3) is absent. For the statistical analysis of KARMEN data we are using the 9 data points as well as the expected background for the prompt energy given in Fig. 11b of Ref. [2].

<sup>4</sup> Note that here we neglected the dependence of the couplings  $g_\alpha$  on the helicity indices due to complex phases in  $U_{\alpha l}$  and  $g_{4l}$  according to Eq. (2.11). If this additional freedom is taken into account, different branching ratios  $R_e$  for the helicity-conserving and helicity-flipping decays can be obtained, which will modify the relative size of the  $\nu_\mu$  line contribution.

In Fig. 2 we show the allowed regions for LSND, KARMEN, and the combination of both experiments for the case of oscillations and for the decay scenario. The comparison of the left and right panels of Fig. 2 shows that the compatibility of LSND and KARMEN in the decay scenario is at the same level as for oscillations. The reason is that both the oscillation phase, and the exponent  $\Gamma_4 L$  in Eq. (3.1), have the same dependence on  $L/E_\nu$ . This allows us to accommodate both the positive signal in the LSND experiment and the KARMEN null result, by taking into account the different baselines ( $L_{\text{LSND}} = 35$  m,  $L_{\text{KARMEN}} = 18$  m). In addition, as discussed above, the  $\nu_\mu$  line gives a small contribution to the LSND signal, which is absent in KARMEN because of the time cut.

A powerful tool to evaluate the compatibility of different data sets is the parameter goodness of fit (PG) criterion discussed in Ref. [37]. It is based on the  $\chi^2$  function

$$\chi_{\text{PG}}^2 = \chi_{\text{tot,min}}^2 - \sum_i \chi_{i,\text{min}}^2, \quad (3.4)$$

where  $\chi_{\text{tot,min}}^2$  is the  $\chi^2$  minimum of all data sets combined and  $\chi_{i,\text{min}}^2$  is the minimum of the data set  $i$ . Applying this method to the case of LSND and KARMEN we find  $\chi_{\text{PG}}^2 = 5.02$  for oscillations and  $\chi_{\text{PG}}^2 = 4.97$  for decay. These  $\chi^2$  numbers have to be evaluated for 2 dof, corresponding to the two parameters in common to the two data sets ( $\sin^2 2\theta$  and  $\Delta m^2$  for oscillations and  $|U_{\mu 4}|^2 R_e$  and  $\bar{g}m_4$  for decay). This yields a PG of 8.1% for oscillations and 8.3% for decay.

#### IV. COMBINED ANALYSIS OF LSND AND NULL-RESULT EXPERIMENTS

Let us now discuss the survival probabilities relevant to the analysis of SBL disappearance experiments. Under the assumption  $U_{e4} = 0$  in Eq. (2.6), no  $\bar{\nu}_e$  disappearance is expected in SBL reactor experiments:  $P_{\bar{\nu}_e \rightarrow \bar{\nu}_e} = 1$ . However, since we need mixing of  $\nu_\mu$  with the heavy states in order to explain the LSND signal, one expects some effect in  $\nu_\mu$  disappearance experiments. To simplify the analysis, we will neglect in the following the appearance of  $\nu_\mu$  in the decay products, i.e. we adopt the choice  $R_e \approx 1$  and  $R_{\mu,\tau} \approx 0$  for the branching ratios of the decay. Then Eq. (2.6) yields for the SBL  $\nu_\mu$  survival probability

$$P_{\nu_\mu \rightarrow \nu_\mu}^{\text{SBL,dec}} = (1 - |U_{\mu 4}|^2)^2 + |U_{\mu 4}|^4 e^{-\Gamma_4 L}. \quad (4.1)$$

In the relevant  $L/E_\nu$  range the most stringent bound on  $\nu_\mu$  disappearance comes from the CDHS experiment [12], where the number of  $\nu_\mu$  events in a near and far detector are compared. Therefore this experiment is only sensitive to the  $L$  dependent term in Eq. (4.1). Since this term enters only via  $|U_{\mu 4}|^4$  the sensitivity of CDHS to  $U_{\mu 4}$  is rather poor in the decay scenario. Eq. (4.1) has to be compared to

$$P_{\nu_\mu \rightarrow \nu_\mu}^{\text{SBL,osc}} = 1 - 4|U_{\mu 4}|^2(1 - |U_{\mu 4}|^2) \sin^2 \frac{\Delta m_{41}^2 L}{4E} \quad (4.2)$$

for oscillations in a (3+1) four-neutrino scheme. In this case  $L$ -dependent effects enter already at order  $|U_{\mu 4}|^2$ , which leads to significantly stronger constraints than in the case of decay. Technical details of our CDHS data analysis can be found in Ref. [38].

As shown in Ref. [39], also atmospheric neutrino data provide a non-trivial bound on the mixing of  $\nu_\mu$  with heavy mass states, i.e. on  $|U_{\mu 4}|^2$ . Following Ref. [39], in the case of (3+1) oscillations, the survival probability of atmospheric  $\nu_\mu$  is given to a good approximation by

$$P_{\nu_\mu \rightarrow \nu_\mu}^{\text{ATM,osc}} \approx P_l + |U_{\mu 4}|^4, \quad (4.3)$$

where  $P_l$  is an effective survival probability involving only oscillations of the light mass states  $m_l$ , which is obtained by numerically solving the evolution equation within the Earth matter. Note that the parameter  $|U_{\mu 4}|^2$  enters also in  $P_l$ . The recent update of a four-neutrino analysis of atmospheric [3], and K2K [5] neutrino data performed in Ref. [11] gives the bound

$$|U_{\mu 4}|^2 \leq 0.065 \quad (99\% \text{ C.L.}), \quad (4.4)$$

which holds for  $m_4 \gg \sqrt{\Delta m_{\text{ATM}}^2} \sim 0.05$  eV, where  $\Delta m_{\text{ATM}}^2$  is the mass-squared difference responsible for atmospheric neutrino oscillations. In the decay scenario the survival probability of atmospheric neutrinos is modified to

$$P_{\nu_\mu \rightarrow \nu_\mu}^{\text{ATM,dec}} \approx P_l + |U_{\mu 4}|^4 e^{-\Gamma_4 L} \approx P_l, \quad (4.5)$$

where in the last step we have used the fact that for decay rates relevant to LSND, we have  $\Gamma_4 L \gg 1$  for atmospheric baseline and energy ranges. Comparing Eqs. (4.3) and (4.5) we find that neglecting the small term  $|U_{\mu 4}|^4$  the constraint obtained for oscillations applies also in the case of decay. Note that the decay will give a small contribution (suppressed by  $|U_{\mu 4}|^2$ ) to the  $P_{\nu_\mu^r \rightarrow \nu_e^s}$  transition probability for atmospheric neutrinos, which potentially affects  $e$ -like events. In addition, in general one has to take into account also oscillations of the decay products with  $\Delta m_{ll'}^2$  for atmospheric neutrinos, and some of the  $\nu_e^r$  produced in the decay will oscillate back to  $\nu_\mu^r$ . However, under the assumption  $R_e \approx 1, R_{\mu,\tau} \approx 0$  for the branching ratios, oscillations of the decay products with  $\Delta m_{\text{ATM}}^2$  will be doubly-suppressed by  $|U_{\mu 4} U_{e 3}|^2$ . In the following decay analysis we will neglect such subleading effects in atmospheric neutrinos, and we will use as an approximation the  $\chi^2(|U_{\mu 4}|^2)$  from Fig. 19 of Ref. [11], which has been obtained for oscillations. A detailed investigation of atmospheric neutrino data within the decay scenario is beyond the scope of the present work.

Now we turn to the global analysis of all SBL data, and we investigate the compatibility of LSND and null-result experiments within the decay scenario. In Fig. 3 we show the allowed regions from the appearance experiments LSND+KARMEN compared with the bound implied from disappearance experiments. In this bound we include data from the  $\bar{\nu}_e \rightarrow \bar{\nu}_e$  reactor experiments Bugey [13], CHOOZ [40], and Palo Verde [41], as well as  $\nu_\mu$  data from CDHS [12], atmospheric neutrinos [3], and the K2K long-baseline experiment [5], as described above.

In the left panel of Fig. 3 we reproduce the well-known result (see e.g. Refs. [38, 39]) that, for (3+1) mass schemes, the effective oscillation amplitude  $\sin^2 2\theta_{\text{eff}} = 4|U_{e 4}|^2|U_{\mu 4}|^2$  is tightly constrained from the disappearance experiments by the quadratic appearance of the small parameters  $|U_{e 4}|^2$  and  $|U_{\mu 4}|^2$ . In contrast, in case of decay, appearance and disappearance experiments are in perfect agreement, as is clear from the right panel of Fig. 3; there is a large overlap of the allowed regions for both data sets. The only relevant constraint from

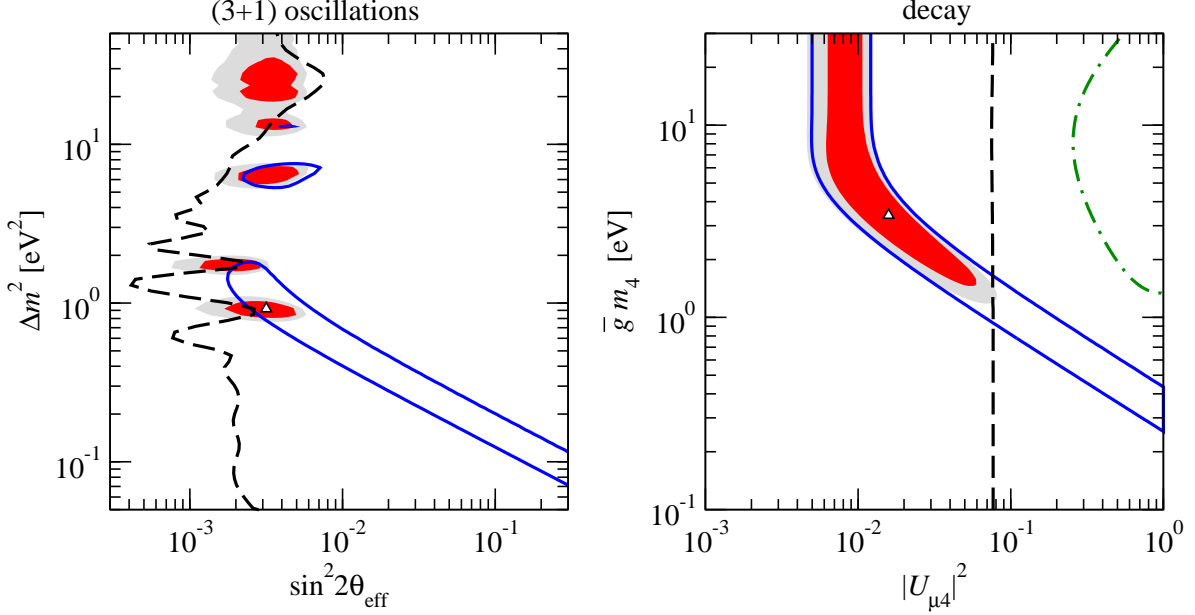


**FIG. 3:** Allowed regions for LSND+KARMEN (solid) and SBL disappearance+atmospheric neutrino experiments (dashed) at 99% CL, and the combination of these data (shaded regions) at 90% and 99% CL. The left panel corresponds to neutrino oscillations in the (3+1) mass scheme and the right panel to the decay scenario presented in this work. The dash-dotted curve in the right panel shows the 99% CL constraint from CDHS.

disappearance data comes from the bound from atmospheric neutrinos shown in Eq. (4.4). As mentioned above no constraint arises from reactor experiments, and in agreement with the discussion related to Eq. (4.1) one can see in Fig. 3 that the constraint from CDHS is too weak to contribute significantly within the decay framework. The shaded regions in the figure show the allowed regions obtained from combining all data, where the total number data points is

$$11_{(\text{LSND})} + 9_{(\text{KARMEN})} + 15_{(\text{CDHS})} + 60_{(\text{Bugey})} + 1_{(\text{CHOOZ})} + 1_{(\text{Palo Verde})} + 1_{(\text{ATM})} = 98. \quad (4.6)$$

The global analysis gives the following best fit parameters for the decay scenario

$$|U_{\mu 4}|^2 = 0.016, \quad \bar{g} m_4 = 3.4 \text{ eV}. \quad (4.7)$$

Hence, for neutrino masses in the range 100 keV coupling constants of order  $10^{-5}$  are sufficient to make the decay fast enough. Let us quantify the quality of the fit further using three different statistical tests.

1. First we compare the fit for oscillations and decay by using the absolute values of the global  $\chi^2$  minimum. We find

$$\chi_{\text{min,osc}}^2 = 96.9, \quad \chi_{\text{min,dec}}^2 = 88.3. \quad (4.8)$$

Although the GOF implied by these numbers is good in both cases, thanks to the large number of data points (see Eq. (4.6)), the  $\Delta\chi^2 = 8.6$  indicates that decay provides a significantly better description of the global data.

2. Next we use the PG [37] to test the compatibility of LSND with the rest of the data. Applying Eq. (3.4) to this case we find

$$\begin{aligned} \text{osc: } \chi_{\text{PG}}^2 &= 21.8, & \text{PG} &= 1.8 \times 10^{-3} \% \\ \text{dec: } \chi_{\text{PG}}^2 &= 6.2, & \text{PG} &= 4.6 \% \end{aligned} \quad (\text{LSND vs rest}) \quad (4.9)$$

where the  $\chi^2$  values have been evaluated for 2 dof corresponding to the two parameters in common to the two data sets. The PG numbers show that for oscillations there is a severe disagreement between LSND and all the other experiments, whereas the PG is acceptable within the decay framework. The reason for the rather small PG even for decay comes from the slight conflict between LSND and KARMEN, which is present in any of the scenarios. Note that for five-neutrino oscillations in a (3+2) mass scheme, a similar analysis performed in Ref. [18] yielded  $\text{PG}_{(3+2)} = 2.1\%$ , slightly worse than the one for decay.

3. The better agreement of the data for decay becomes even more transparent if we test the compatibility of appearance and disappearance experiments, i.e. similar to Fig. 3, we divide the global data into LSND+KARMEN and all the rest. Then the PG analysis gives

$$\begin{aligned} \text{osc: } \chi_{\text{PG}}^2 &= 16.6, & \text{PG} &= 2.5 \times 10^{-2} \% \\ \text{dec: } \chi_{\text{PG}}^2 &= 1.2, & \text{PG} &= 55 \% \end{aligned} \quad (\text{app. vs disapp.}) \quad (4.10)$$

In this analysis the conflict between LSND and KARMEN is removed, since they are added up to one single data set. Therefore, the above numbers confirm our conclusion from Fig. 3 that appearance and disappearance experiments are in perfect agreement in the decay scenario.

Before concluding this Section, let us mention again that we have performed the analysis by setting  $U_{e4} = 0$  and  $R_e = 1, R_\mu = 0$ . This reduces the number of parameters, and hence simplifies the analysis considerably. Although we do not expect a significant change of our results by relaxing these assumptions, we stress that on general grounds this can only *improve* the fit of the decay scenario, since more parameters become available to describe the data.

## V. PREDICTIONS FOR MINIBOONE AND OTHER FUTURE EXPERIMENTS

### A. MiniBooNE

A critical test of the LSND signal will come from the MiniBooNE experiment [24], which is currently taking data. This experiment looks for  $\nu_e$  appearance in a beam of  $\nu_\mu$  neutrinos with a mean energy of  $\sim 700$  MeV at a baseline of  $L \simeq 540$  m. In the minimal decay framework discussed in the previous Sections we predict for MiniBooNE the appearance of  $\nu_e$  events with a probability of the same order as in LSND, similar to the case of oscillations. Since the MiniBooNE detector cannot distinguish between neutrinos and antineutrinos, the

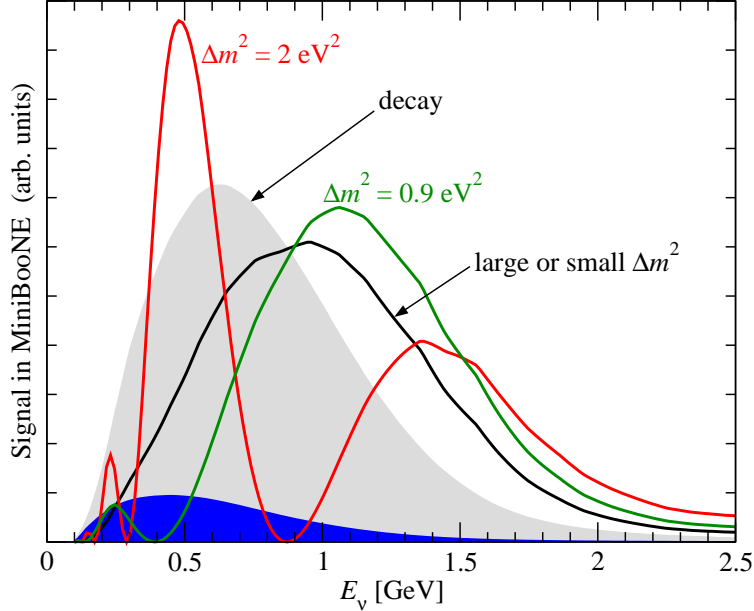


**FIG. 4:** Energy spectrum predicted for the  $\nu_e$  appearance signal in MiniBooNE for decay with  $\bar{g}m_4 = 3.4$  eV (shaded region) and for various values of  $\Delta m^2$  in the case of oscillations (solid curves). The blue/dark-shaded region shows the contribution of  $\bar{\nu}_e$  from the helicity changing decay.

$\bar{\nu}_e$  produced in the helicity-flipping decay  $n_4 \rightarrow \bar{\nu}_e \phi$  will also contribute to the signal. We calculate the differential number of events as

$$\frac{dN}{dE_{\nu_e}} \propto \int_{E_{\nu_e}}^{\infty} dE_{\nu_\mu} \phi(E_{\nu_\mu}) \left[ \frac{dP_{\nu_\mu \rightarrow \nu_e}(E_{\nu_\mu})}{dE_{\nu_e}} \sigma(E_{\nu_e}) + \frac{dP_{\nu_\mu \rightarrow \bar{\nu}_e}(E_{\nu_\mu})}{dE_{\bar{\nu}_e}} \bar{\sigma}(E_{\nu_e}) \right], \quad (5.1)$$

where  $\sigma$  ( $\bar{\sigma}$ ) is the total charged-current cross section for neutrinos (antineutrinos), and  $\phi(E_{\nu_\mu})$  is the initial flux of  $\nu_\mu$ , which we extract from Fig. 3 of Ref. [24].

The spectral shape predicted by Eq. (5.1) is shown in Fig. 4. Although the heavy neutrino mass state decays with equal probability into  $\nu_e$  and  $\bar{\nu}_e$ , the antineutrinos give only a small contribution to the total signal. The reason is that, according to Eq. (2.7), most of the decay products from the helicity-flipping decay will have low energies, for which the detection cross section is small. Moreover, the detection cross section for antineutrinos is roughly a factor two smaller than the one for neutrinos. Note that the spectral distortion implied by  $W_{rs}(E_{\nu_\alpha}, E_{\nu_\beta})$  will be less pronounced in MiniBooNE than in LSND because of the very different initial spectra. In the LSND experiment, the spectrum rises monotonically up to a maximum energy, whereas the MiniBooNE spectrum decreases with energy. Therefore, degrading the energy of the decay products has a smaller impact on the final spectrum in the case of MiniBooNE.

In Fig. 4 we show also the predicted spectral shape in the case of oscillations for several values of  $\Delta m^2$ . One observes that in principle the decay predicts a specific spectral shape of the signal, whereas the actual spectrum from oscillations depends strongly on  $\Delta m^2$ . Whether it will be possible to distinguish between the two models in the case of a positive signal in MiniBooNE depends on the available statistics, as well as on experimental factors such as

the energy resolution for  $E_\nu$ , which are not taken into account in Fig. 4.

Another method to discriminate between decay and oscillations is provided by the disappearance channel in MiniBooNE. In the case of (3+1), as well as (3+2) oscillations sizeable  $\nu_\mu$  disappearance is predicted, which should be observable in MiniBooNE [42]. In contrast, the signal is expected to be very small in the decay scenario. The disappearance search in MiniBooNE is limited to a shape analysis of the energy spectrum, since the normalisation of the total number of events suffers from large uncertainties [42]. Therefore, the signal for decay is suppressed for the same reason as discussed above in relation with Eq. (4.1) and the CDHS experiment.

### B. Experiments looking for a non-zero value of $U_{e3}$

In general the decay will contribute to the signal in experiments such as T2K [43] or NO $\nu$ A [44] looking for a non-zero value of  $U_{e3}$  by exploring the channel  $\nu_\mu \rightarrow \nu_e$ . However, the appearance probability would be proportional to  $|U_{\mu 4}|^2 \sim 0.01$ , and thus at the edge of the sensitivity for those experiments. Therefore, it appears to be rather challenging first to observe an effect of our decay scenario, and second to disentangle it from oscillations induced by  $U_{e3}$ . Much as in MiniBooNE, the signal from decay will have a characteristic spectral shape, as implied by the spectrum of the decay products. Moreover, in detectors capable of distinguishing neutrinos from antineutrinos the appearance of “wrong-helicity” neutrinos with low energies would be a generic prediction of the decay scenario. Nevertheless, this is also very challenging, because charge discrimination for electrons is a difficult experimental task. In this respect, an interesting possibility to explore the decay scenario might be to look for the appearance of  $\bar{\nu}_e$  from the  $\nu_\mu$  beam of T2K in the KamLAND detector. Let us note that also the Minerva experiment [45], which will be placed  $\sim 1$  km away from the target within the NuMI neutrino beam, or the K2K/T2K near detectors could be suitable places to look at these effects, although these beams might suffer from a large intrinsic  $\nu_e$  ( $\bar{\nu}_e$ ) background.

Another manifestation of the decay model could be the observation of  $\nu_\mu \rightarrow \nu_e$  appearance in accelerator experiments such as T2K or NO $\nu$ A, but no corresponding signal for  $\bar{\nu}_e$  disappearance in reactor experiments such as Double-Chooz [46]. This would imply very small values of  $U_{e3}$ , such that  $\bar{\nu}_e$  disappearance is suppressed, whereas the  $\nu_\mu \rightarrow \nu_e$  appearance signal is dominated by the decay. Note, however, that a positive signal for  $\bar{\nu}_e$  disappearance in reactor experiments cannot exclude the decay scenario, since our model is perfectly compatible with a sizeable value of  $U_{e3}$ .

In summary, we stress that a direct measurement of the decay effects is quite challenging for present and near-future experiments looking for a non-zero value of  $U_{e3}$ , because of the rather small mixing,  $|U_{\mu 4}|^2$ , which is needed in order to accommodate the LSND result. Therefore, if the LSND signal should be confirmed by MiniBooNE a new experiment at a stopped pion neutrino source as proposed in Ref. [47] could be an optimal experiment to confirm or exclude our decay model.

## VI. CP-VIOLATING DECAYS AND THE SIGNAL IN MINIBOONE

In this Section we extend our model and consider the case of two heavy neutrinos, i.e.  $N = 5$  massive neutrinos. We will show that in this case it is possible to obtain an interference between oscillation and decay amplitudes [35], which may lead to CP violation in the decay. In this way the signal in MiniBooNE (running in the neutrino mode) can be significantly suppressed with respect to the LSND signal from antineutrinos.

Using Eq. (2.8) for  $N = 5$  and performing the integral over  $L$ , one finds

$$\begin{aligned}
 P_{\nu_\alpha \rightarrow \nu_\beta}^{\text{dec}} &\equiv \int_0^L dL' \frac{dP_{\nu_\alpha \rightarrow \nu_\beta}^{\text{dec}}}{dL'} \\
 &= \sum_h \frac{1}{2} |U_{\alpha h}|^2 R_{h\beta} (1 - e^{-\Gamma_h L}) \\
 &\quad + \bar{R}_\beta |U_{\alpha 4}| |U_{\alpha 5}| \cos \gamma \left[ \cos(\delta + \gamma) - e^{-\bar{\Gamma} L} \cos(\delta + \gamma + \Gamma_{\text{osc}} L) \right], \quad (6.1)
 \end{aligned}$$

with the following definitions for the branching ratios

$$R_{h\beta} \equiv 2 \frac{|g_{h\beta}|^2 A_h^2}{\Gamma_h}, \quad \bar{R}_\beta \equiv 2 \frac{|g_{4\beta}| |g_{5\beta}| A_4 A_5}{\bar{\Gamma}}, \quad \bar{\Gamma} \equiv \frac{\Gamma_4 + \Gamma_5}{2}, \quad (6.2)$$

and phases

$$\delta \equiv \arg(U_{\alpha 4}^* U_{\alpha 5} g_{4\beta} g_{5\beta}^*), \quad \tan \gamma \equiv \frac{\Gamma_{\text{osc}}}{\bar{\Gamma}}, \quad \Gamma_{\text{osc}} \equiv \frac{\Delta m_{54}^2}{2E_{\nu_\alpha}}. \quad (6.3)$$

The first term in Eq. (6.1) describes the incoherent decay of the two heavy mass states in analogy to Eq. (3.1), whereas the second term results from the interference of the amplitudes for decay and oscillations of the two heavy neutrino mass states  $n_4$  and  $n_5$ . The phase  $\delta$  is the analogue of the Dirac phase leading to CP violation in the standard three neutrino oscillation framework. In fact, in the case of antineutrinos,  $U_{\alpha h}$  and  $g_{h\beta}$  have to be replaced by  $U_{\alpha h}^*$  and  $g_{h\beta}^*$ , which implies  $\delta \rightarrow -\delta$ , and we obtain the CP asymmetry:

$$\begin{aligned}
 \Delta P &\equiv P_{\bar{\nu}_\alpha \rightarrow \bar{\nu}_\beta}^{\text{dec}} - P_{\nu_\alpha \rightarrow \nu_\beta}^{\text{dec}} \\
 &= 2\bar{R}_\beta |U_{\alpha 4}| |U_{\alpha 5}| \cos \gamma \sin \delta \left[ \sin \gamma - e^{-\bar{\Gamma} L} \sin(\gamma + \Gamma_{\text{osc}} L) \right]. \quad (6.4)
 \end{aligned}$$

One observes that necessary conditions to obtain CP violation are  $\delta \neq 0, \pi$  and  $\tan \gamma \sim 1$ , i.e.  $\bar{\Gamma} \sim \Gamma_{\text{osc}}$  or  $\bar{g}_h^2 m_h^2 / 8\pi \sim \Delta m_{54}^2$ . Using  $\bar{g}_h m_h \sim \text{few eV}$ , the last condition shows that the heavy neutrinos ( $m_h > \text{keV}$ ) have to be highly degenerate.

In Fig. 5 we show a numerical example for the  $P_{\bar{\nu}_\mu \rightarrow \bar{\nu}_e}^{\text{dec}}$  and  $P_{\nu_\mu \rightarrow \nu_e}^{\text{dec}}$  transition probabilities for an  $L/E_\nu$  value relevant to LSND and MiniBooNE. Clearly, in this example the neutrino signal is strongly suppressed with respect to the antineutrino signal for  $\Delta m_{54}^2 \sim 1 \text{ eV}^2$ . This result confirms the previous observation that in order to obtain CP violation, the two heavy neutrinos have to be very degenerate, with masses in the keV range and a mass difference in the eV range. Whether this mechanism allows indeed to accommodate the LSND signal with a possible null-result of the MiniBooNE experiment in the neutrino mode has to be investigated after the release of the MiniBooNE data by a combined analysis of the two experiments within this framework. In that case, MiniBooNE data taking with an antineutrino beam would be necessary in order to test the CP-violating decay scenario.

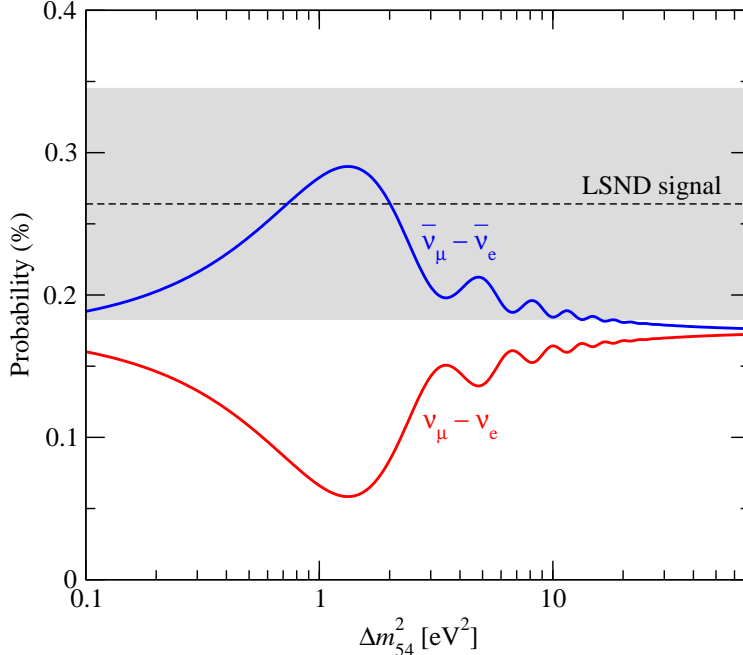


**FIG. 5:** The transition probabilities  $P_{\bar{\nu}_\mu \rightarrow \bar{\nu}_e}^{\text{dec}}$  and  $P_{\nu_\mu \rightarrow \nu_e}^{\text{dec}}$  according to Eq. (6.1). The shaded region corresponds to the  $1\sigma$  range for  $P_{\bar{\nu}_\mu \rightarrow \bar{\nu}_e}$  observed in LSND. The chosen parameter values are  $L/E_\nu \simeq 0.75$  m/MeV,  $|U_{\mu 4}|^2 = |U_{\mu 5}|^2 = 0.003$ ,  $R_{4e} = R_{5e} = \bar{R}_e = 1$ ,  $\Gamma_4 = \Gamma_5 = \bar{\Gamma}$  with  $\bar{g}_h m_h = 3.4$  eV, and  $\delta = \pi/2$ .

## VII. CONSTRAINTS FROM LABORATORY, COSMOLOGY, AND ASTROPHYSICS

Mixing between active and sterile neutrinos<sup>5</sup>, and couplings between active neutrinos and a light scalar, have been extensively studied, both in laboratory experiments and, for their implications in the evolution of the early Universe and of supernovae. For the discussion of these constraints we will focus on the minimal scenario necessary to explain the LSND signal: we require only mixing of  $\nu_\mu$  with the heavy mass state,  $|U_{\mu 4}|^2 \sim 0.01$ , whereas we set  $U_{e4} = U_{\tau 4} = 0$ . Furthermore, the assumption  $R_e = 1, R_{\mu, \tau} = 0$  for the branching ratios of the decay implies that only two elements of the (symmetric) coupling matrix in the flavour basis,  $g_{\alpha\beta}$ , are non-zero:  $g_{es} \simeq \bar{g}$  and  $g_{e\mu} \simeq U_{\mu 4} \bar{g}$ .

First we note that in our model solar neutrino oscillations are completely unaffected. Because of the assumption  $U_{e4} = 0$ , no  $n_h$  component can be produced in the Sun, and since the  $\nu_l$  in our scenario are stable, there is no decay of solar neutrinos. For the very same reason the decay has also no effect in the KamLAND experiment, and these data are entirely explained by oscillations of the light neutrinos. On the other hand, effects in atmospheric neutrino experiments have been discussed in Section IV.

<sup>5</sup> See Ref. [48] for a recent analysis of various bounds on sterile neutrino mixing.

## A. Laboratory bounds

In general, the mixing of a heavy neutrino leads to contributions to the effective neutrino masses in neutrinoless double-beta decay [49] and tritium beta decay [50] experiments. Note, however, that in our scenario there will be no effect of the heavy neutrino in such experiments because of our assumption  $U_{e4} = 0$ . The coupling between  $\nu_e$  and a light scalar would induce double-beta decay with the emission of one or two scalars, with a spectrum for the two electrons which is distinguishable from the one of the two-neutrino double-beta decay. Relatively strong bounds for single scalar emission [51] apply only to the coupling  $g_{ee}$ , which can be arbitrary small in our scenario. The couplings  $g_{e\alpha}$  for  $\alpha \neq e$  contribute in principle to double-beta decay with the emission of two scalars. However, in this case the limits are very weak [51]:  $g < \mathcal{O}(1)$ .

The decay of pions and kaons has been used to set bounds on the mixing of heavy neutrinos (see Ref. [32] and references therein). If a massive neutrino with  $m_h \gg m_{1,2,3}$  were produced in such decays, the energy spectrum of the muon would present an additional monochromatic line. No positive signal was found, leading to strong constraints on the mixing for neutrino with masses  $m_h \gtrsim 1$  MeV. Mixing of neutrinos with smaller masses are compatible with these bounds. Furthermore, light scalar emission was not observed in pion and kaon decays [52, 53]. The most stringent bounds are of order  $g^2 < \text{few} \times 10^{-5}$ , much too weak to constrain our model.

## B. Supernova bounds

To estimate the effect of our model in thermal environments such as in a supernova and the early Universe let us compare the rate of processes induced by the Lagrangian Eq. (2.1) to the one of weak processes of the type  $\nu e \rightarrow \nu e$ . From dimensional considerations, it follows that  $\sigma_{\text{weak}} \sim G_F^2 E^2$ , where  $E$  is the typical energy of the involved particles. Using  $\sigma(2 \leftrightarrow 1) \sim \bar{g}^2 m_h^2 / E^4$  and  $\sigma(2 \leftrightarrow 2) \sim \bar{g}^4 / E^2$ , where  $2 \leftrightarrow 1$  denotes processes like  $\nu_l \phi \leftrightarrow n_h$ ,  $\nu_l n_h \rightarrow \phi$ , and  $2 \leftrightarrow 2$  indicates processes like  $\nu_l \nu_l \leftrightarrow \phi \phi$ ,  $\nu_l \nu_l \leftrightarrow n_h n_h$ , we find<sup>6</sup>

$$\frac{\sigma(2 \leftrightarrow 1)}{\sigma_{\text{weak}}} \sim 10^{10} \left( \frac{\bar{g} m_h}{1 \text{ eV}} \right)^2 \left( \frac{E}{1 \text{ MeV}} \right)^{-6}, \quad (7.1)$$

$$\frac{\sigma(2 \leftrightarrow 2)}{\sigma_{\text{weak}}} \sim 10^2 \left( \frac{\bar{g}}{10^{-5}} \right)^4 \left( \frac{E}{1 \text{ MeV}} \right)^{-4}. \quad (7.2)$$

In addition to these reactions induced by the scalar coupling, heavy mostly-sterile neutrinos are produced via oscillations due to their mixing with the active ones.

If heavy neutrinos and light scalars were produced in the core of a supernova and could escape freely, they would carry away a large amount of energy, substantially modifying the supernova evolution. Together with the observations from supernova SN1987A, this energy-loss argument has been used to constrain sterile neutrino mixing [54] as well as Majoron

---

<sup>6</sup> For a careful analysis of these processes for active neutrinos see Ref. [33].

coupling, see e.g. Refs. [33, 55]. In our scenario the mass of the heavy neutrino is large compared with the matter potential within the supernova core. Therefore, we can treat mixing, as well as the reactions involving the scalar and  $n_h$ , as in vacuum. From Eq. (7.1) it follows that for typical energies in the supernova cores,  $E \sim 10$  MeV,  $2 \leftrightarrow 1$  reactions are  $10^4$  times faster than weak interactions. This implies that  $n_h$  and  $\phi$  are strongly coupled to the active neutrinos, and hence, they are trapped within the neutrinosphere, avoiding any energy loss due to particles escaping from the core. Let us add that there might be additional effects, such as modification of lepton number or neutrino flux distortions [53, 56]. The analysis of such effects requires detailed studies, which are beyond the scope of the present work.

### C. Cosmological bounds

Constraints on the number of relativistic degrees of freedom present at the time of Big Bang Nucleosynthesis (BBN), usually parametrized by the number of neutrino flavours  $N_\nu$ , are relevant when light particles such as sterile neutrinos are introduced [57]. Analyses of cosmological data, including light-element abundances lead to the limits  $2.3 \leq N_\nu \leq 3.0$  (95% CL) [58]. A recent analysis, that uses a new assessment of the primordial  ${}^4\text{He}$  abundance and its uncertainty, has substantially relaxed the bounds on  $N_\nu \geq 3$ :  $\delta N_\nu \leq 1.44$  (95% CL) [59], where  $\delta N_\nu \equiv N_\nu - 3$ . The discrepancy between these two exemplary results illustrates that such bounds have to be considered with care, because of the systematical uncertainties in light-element abundances, and the dependence on input priors.

In the early Universe,  $n_h$  of our decay model are initially generated by mixing with active neutrinos [60]. As soon as  $n_h$  are produced, they are thermalized together with the scalar due to the very fast  $2 \leftrightarrow 1$  reactions. Hence, one additional neutrino and one scalar degree of freedom will be present during BBN, leading to  $N_\nu = 4.57$ , which appears to be disfavoured by the limits quoted above.<sup>7</sup> However, to draw reliable conclusions from BBN considerations a more detailed analysis is required, since there are many effects which might play a role. For example, in the presence of a small chemical potential for  $\nu_e$  the limit on extra relativistic degrees of freedom becomes much weaker,  $N_\nu \leq 6.5$  [58], and hence  $N_\nu = 4.57$  is allowed. Moreover, a detailed simulation of BBN in the presence of  $\tau$ -neutrino decay performed in Ref. [61] showed that the effective  $N_\nu$  depends in a rather non-trivial way on model parameters, and values of  $\delta N_\nu > 0$  as well as  $< 0$  may be obtained. Let us mention also the possibility to avoid the thermalization of  $n_h$  and  $\phi$  at BBN, by suppressing the initial production of  $n_h$  through mixing. This could be achieved e.g. through a large lepton asymmetry of order  $10^{-3}$  [62], a matter potential induced by neutrino–Majoron interactions [63], or by assuming a low reheating temperature [20]. The  $2 \leftrightarrow 2$  processes would not be efficient in producing and thermalizing sterile neutrinos and scalars as far as they are slower than the expansion rate at BBN. Couplings  $g \lesssim \text{few} \times 10^{-6}$  guarantee that these scatterings are out of equilibrium for  $T \gtrsim 100$  keV (see Eq. (7.2)).

---

<sup>7</sup> Note that also in four- or five-neutrino oscillation schemes the sterile neutrinos are thermalized within the standard BBN scenario [57].

As can be seen from Eqs. (7.1) and (7.2) the scalar interactions have a recoupling form, instead of the usual decoupling form of weak interactions, i.e. their strength grows as the Universe evolves, which may have some effects in later epochs of the Universe. For instance, if a light scalar couples to neutrinos before the recombination era, effects like a delayed matter–radiation equality and enhanced damping of acoustic oscillations at higher  $l$  can occur because the radiation energy density differs from that of the standard scenario. Moreover, if one or more neutrinos are scattering during the eV era rather than free-streaming, a uniform shift of the CMB peaks to larger  $l$  would be manifest [64].

Finally, we note that our scenario, with the scalar heavier than the light neutrinos, does not give rise to a neutrinoless Universe [65], which is disfavoured by structure formation arguments [66].

## VIII. SUMMARY AND CONCLUSIONS

We have presented an explanation for the LSND evidence for  $\bar{\nu}_e$  appearance based on the decay of a heavy sterile neutrino into a light scalar particle and light neutrinos. We assume a small mixing of the heavy neutrino mass eigenstate  $n_4$  with  $\nu_\mu$  of order  $|U_{\mu 4}|^2 \sim 0.01$ , such that a small  $n_4$  component is contained in the initial  $\bar{\nu}_\mu$  beam produced in the LSND experiment. On the way to the LSND detector the  $n_4$  decays into the scalar and a superposition of light neutrino mass eigenstates. If this final state contains a large fraction of the  $\bar{\nu}_e$  flavour, it will give rise to the  $\bar{\nu}_e$  appearance signal observed in LSND. Taking into account the energy distribution of the decay products, one obtains a characteristic prediction for the spectral shape of the LSND signal, with more events at the lower part of the spectrum. Comparing this prediction with the spectral data of LSND, we find that the fit of the decay is slightly worse than for oscillations, although still acceptable ( $\chi^2_{\text{decay}} = 10.8/9$  dof). A more detailed investigation of the LSND spectral data might allow to distinguish between decay and oscillations.

We have performed a global fit to all relevant data, including null-result short-baseline reactor and accelerator oscillation experiments. The agreement of the  $\bar{\nu}_\mu \rightarrow \bar{\nu}_e$  appearance experiments LSND and KARMEN in the decay scenario is at the same level as in the case of oscillations. Much as the oscillation phase, also the decay exponential depends on  $L/E_\nu$ , which allows us to reconcile the two results due to the different baselines. However, unlike the case of (3+1) four-neutrino schemes, our decay model is in complete agreement with the constraints from disappearance results. Using the so-called parameter goodness of fit (PG) to test the compatibility of appearance (LSND, KARMEN) and disappearance (Bugey, CHOOZ, CDHS, atmospheric neutrino) experiments, we find PG = 55% for decay but only PG = 0.025% for (3+1) oscillations. Testing the compatibility of LSND and all the null-result experiments, we find PG = 4.6% for decay, which is slightly better than the PG = 2.1% obtained in Ref. [18] for a (3+2) five-neutrino oscillation scenario. In addition, we have shown that our model is consistent with present laboratory bounds and have discussed implications for supernova evolution, BBN and CMB observations.

In the minimal version of the decay model we predict a signal in the upcoming MiniBooNE experiment corresponding to a transition probability of the same order as seen in LSND, and

we have discussed characteristic signatures of our scenario, which may allow to distinguish it from oscillations in MiniBooNE or other future neutrino experiments. Furthermore, we have shown that within an extension of the minimal decay model it is possible to introduce CP violation in the decay through an interference term between decay and oscillations of two nearly degenerate heavy neutrinos, with masses in the 1 keV–1 MeV range and  $\Delta m_{54}^2 \sim 1 \text{ eV}^2$ . This can lead to a suppression of the signal in MiniBooNE running in the neutrino mode, and simultaneously accounting for the antineutrino signal in LSND. Hence, this model can only be excluded if MiniBooNE does not find a positive signal either in the neutrino mode or running with antineutrinos.

### Acknowledgements

We thank J. Beacom, B. Louis, S. Pakvasa, S. Pastor, S.T. Petcov, H. Ray, R. Scherrer, M. Sorel, R. Tomas and W. Winter for useful discussions. S.P.R. and S.P. are grateful to the Fermilab Theoretical Astrophysics Group for kind hospitality during part of this work. T.S. acknowledges support from the CERN Theory group for a visit during which this work was initiated. S.P.R. is supported by NASA Grant ATP02-0000-0151 and by the Spanish Grant FPA2002-00612 of the MCT. T.S. is supported by a “Marie Curie Intra-European Fellowship within the 6th European Community Framework Programme”.

- 
- [1] A. Aguilar *et al.* [LSND Coll.], Phys. Rev. D **64**, 112007 (2001) [hep-ex/0104049].
  - [2] B. Armbruster *et al.* [KARMEN Coll.], Phys. Rev. D **65**, 112001 (2002) [hep-ex/0203021].
  - [3] Y. Fukuda *et al.* [Super-Kamiokande Coll.], Phys. Rev. Lett. **81**, 1562 (1998) [hep-ex/9807003]; Y. Ashie *et al.*, Phys. Rev. D **71**, 112005 (2005) [hep-ex/0501064].
  - [4] Y. Ashie *et al.* [Super-K Coll.], Phys. Rev. Lett. **93**, 101801 (2004) [hep-ex/0404034].
  - [5] E. Aliu *et al.* [K2K Coll.], Phys. Rev. Lett. **94**, 081802 (2005) [hep-ex/0411038].
  - [6] Q. R. Ahmad *et al.* [SNO Coll.], Phys. Rev. Lett. **89**, 011301 (2002) [nucl-ex/0204008]; B. Aharmim *et al.*, nucl-ex/0502021.
  - [7] T. Araki *et al.* [KamLAND Coll.], Phys. Rev. Lett. **94**, 081801 (2005) [hep-ex/0406035].
  - [8] J. T. Peltoniemi, D. Tommasini and J. W. F. Valle, Phys. Lett. B **298**, 383 (1993); J. T. Peltoniemi and J. W. F. Valle, Nucl. Phys. B **406**, 409 (1993) [hep-ph/9302316]; D.O. Caldwell and R.N. Mohapatra, Phys. Rev. D **48**, 3259 (1993).
  - [9] M. Maltoni *et al.*, Nucl. Phys. B **643**, 321 (2002) [hep-ph/0207157].
  - [10] A. Strumia, Phys. Lett. B **539**, 91 (2002) [hep-ph/0201134].
  - [11] M. Maltoni *et al.*, New J. Phys. **6**, 122 (2004) [hep-ph/0405172].
  - [12] F. Dydak *et al.*, Phys. Lett. B **134**, 281 (1984).
  - [13] Y. Declais *et al.*, Nucl. Phys. B **434**, 503 (1995).
  - [14] P. Astier *et al.* [NOMAD Coll.], Phys. Lett. B **570**, 19 (2003) [hep-ex/0306037].
  - [15] E. Ma, G. Rajasekaran and I. Stancu, Phys. Rev. D **61**, 071302 (2000) [hep-ph/9908489]; E. Ma and G. Rajasekaran, Phys. Rev. D **64**, 117303 (2001) [hep-ph/0107203].

- [16] H. Murayama and T. Yanagida, Phys. Lett. B **520**, 263 (2001) [hep-ph/0010178]; G. Barenboim, L. Borissoff and J. Lykken, hep-ph/0212116; M. C. Gonzalez-Garcia, M. Maltoni and T. Schwetz, Phys. Rev. D **68**, 053007 (2003) [hep-ph/0306226].
- [17] K. S. Babu and S. Pakvasa, hep-ph/0204236; B. Armbruster *et al.* [KARMEN Coll.], Phys. Rev. Lett. **90**, 181804 (2003) [hep-ex/0302017]; A. Gaponenko *et al.* [TWIST Coll.], Phys. Rev. D **71**, 071101 (2005) [hep-ex/0410045].
- [18] M. Sorel, J. M. Conrad and M. Shaevitz, Phys. Rev. D **70**, 073004 (2004) [hep-ph/0305255].
- [19] V. Barger, D. Marfatia and K. Whisnant, Phys. Lett. B **576**, 303 (2003) [hep-ph/0308299].
- [20] G. Gelmini, S. Palomares-Ruiz and S. Pascoli, Phys. Rev. Lett. **93**, 081302 (2004) [astro-ph/0403323].
- [21] G. Barenboim and N. E. Mavromatos, JHEP **0501**, 034 (2005) [hep-ph/0404014].
- [22] D. B. Kaplan, A. E. Nelson and N. Weiner, Phys. Rev. Lett. **93**, 091801 (2004) [hep-ph/0401099]; K. M. Zurek, JHEP **0410**, 058 (2004) [hep-ph/0405141].
- [23] H. Paes, S. Pakvasa and T. J. Weiler, hep-ph/0504096.
- [24] J. Monroe [MiniBooNE Coll.], hep-ex/0406048.
- [25] Y. Chikashige, R. N. Mohapatra and R. D. Peccei, Phys. Rev. Lett. **45**, 1926 (1980) and Phys. Lett. B **98**, 265 (1981); G. B. Gelmini and M. Roncadelli, Phys. Lett. B **99**, 411 (1981); H. M. Georgi, S. L. Glashow and S. Nussinov, Nucl. Phys. B **193**, 297 (1981); G. B. Gelmini and J. W. F. Valle, Phys. Lett. B **142**, 181 (1984); A. Santamaria and J. W. F. Valle, Phys. Rev. Lett. **60**, 397 (1988); S. Bertolini and A. Santamaria, Nucl. Phys. B **310**, 714 (1988).
- [26] A. Acker, A. Joshipura and S. Pakvasa, Phys. Lett. B **285**, 371 (1992).
- [27] V. D. Barger *et al.*, Phys. Rev. Lett. **82**, 2640 (1999) [astro-ph/9810121]; P. Lipari and M. Lusignoli, Phys. Rev. D **60**, 013003 (1999) [hep-ph/9901350]; G. L. Fogli *et al.*, Phys. Rev. D **59**, 117303 (1999) [hep-ph/9902267]; S. Choubey and S. Goswami, Astropart. Phys. **14**, 67 (2000) [hep-ph/9904257]; V. D. Barger *et al.*, Phys. Lett. B **462**, 109 (1999) [hep-ph/9907421].
- [28] J. N. Bahcall, N. Cabibbo and A. Yahil, Phys. Rev. Lett. **28**, 316 (1972); S. Pakvasa and K. Tennakone, Phys. Rev. Lett. **28**, 1415 (1972); J. N. Bahcall *et al.*, Phys. Lett. B **181**, 369 (1986); S. Choubey, S. Goswami and D. Majumdar, Phys. Lett. B **484**, 73 (2000) [hep-ph/0004193]; A. Bandyopadhyay, S. Choubey and S. Goswami, Phys. Rev. D **63**, 113019 (2001) [hep-ph/0101273]; J. F. Beacom and N. F. Bell, Phys. Rev. D **65**, 113009 (2002) [hep-ph/0204111].
- [29] B. Armbruster *et al.* [KARMEN Coll.], Phys. Lett. B **348**, 19 (1995).
- [30] K. Eitel [KARMEN Coll.], Nucl. Phys. Proc. Suppl. **91**, 191 (2000) [hep-ex/0008002].
- [31] R. E. Shrock, Phys. Rev. D **24**, 1275 (1981); N. De Leener-Rosier *et al.*, Phys. Rev. D **43**, 3611 (1991); M. Daum *et al.*, Phys. Lett. B **361**, 179 (1995); J. A. Formaggio *et al.* [NuTeV Coll.], Phys. Rev. Lett. **84**, 4043 (2000) [hep-ex/9912062]; M. Daum *et al.*, Phys. Rev. Lett. **85**, 1815 (2000) [hep-ex/0008014].
- [32] A. Kusenko, S. Pascoli and D. Semikoz, hep-ph/0405198.
- [33] Y. Farzan, Phys. Rev. D **67**, 073015 (2003) [hep-ph/0211375].
- [34] C. W. Kim and W. P. Lam, Mod. Phys. Lett. A **5**, 297 (1990); C. Giunti *et al.*, Phys. Rev. D **45** (1992) 1557.
- [35] M. Lindner, T. Ohlsson and W. Winter, Nucl. Phys. B **607**, 326 (2001) [hep-ph/0103170] and

- ibid.* B **622**, 429 (2002) [astro-ph/0105309].
- [36] E. D. Church *et al.*, Phys. Rev. D **66**, 013001 (2002) [hep-ex/0203023].
  - [37] M. Maltoni and T. Schwetz, Phys. Rev. D **68**, 033020 (2003) [hep-ph/0304176].
  - [38] W. Grimus and T. Schwetz, Eur. Phys. J. C **20**, 1 (2001) [hep-ph/0102252].
  - [39] S. M. Bilenky *et al.*, Phys. Rev. D **60**, 073007 (1999) [hep-ph/9903454]; M. Maltoni, T. Schwetz and J. W. F. Valle, Phys. Lett. B **518**, 252 (2001) [hep-ph/0107150] and Phys. Rev. D **65**, 093004 (2002) [hep-ph/0112103].
  - [40] M. Apollonio *et al.*, Eur. Phys. J. C **27**, 331 (2003) [hep-ex/0301017].
  - [41] F. Boehm *et al.*, Phys. Rev. D **64**, 112001 (2001) [hep-ex/0107009].
  - [42] M. Sorel, PhD thesis, FERMILAB-THESIS-2005-07, available at <http://library.fnal.gov/archive/thesis/fermilab-thesis-2005-07.shtml>
  - [43] Y. Itow *et al.*, hep-ex/0106019; T. Kobayashi, talk at NNN05, 7–9 April 2005, Aussois, Savoie, France, <http://nnn05.in2p3.fr/schedule.html>
  - [44] D. S. Ayres *et al.* [NOvA Coll.], hep-ex/0503053.
  - [45] D. Drakoulakos *et al.* [Minerva Coll.], hep-ex/0405002.
  - [46] F. Ardellier *et al.*, hep-ex/0405032; K. Anderson *et al.*, hep-ex/0402041; P. Huber *et al.*, Nucl. Phys. B **665**, 487 (2003) [hep-ph/0303232].
  - [47] G. T. Garvey *et al.*, hep-ph/0501013.
  - [48] M. Cirelli *et al.*, Nucl. Phys. B **708**, 215 (2005) [hep-ph/0403158].
  - [49] H.V. Klapdor-Kleingrothaus *et al.*, Nucl. Phys. Proc. Suppl. **100**, 309 (2001); P. Benes *et al.*, Phys. Rev. D **71**, 077901 (2005) [hep-ph/0501295].
  - [50] V. Lobashev *et al.*, Nucl. Phys. B (Proc. Suppl.) **91**, 280 (2001); C. Weinheimer *et al.*, Nucl. Phys. Proc. Suppl. **118**, 279 (2003).
  - [51] D. Dassié *et al.*, Nucl. Phys. A **678**, 341 (2000).
  - [52] D. I. Britton *et al.*, Phys. Rev. D **49**, 28 (1994); V. D. Barger, W. Y. Keung and S. Pakvasa, Phys. Rev. D **25**, 907 (1982).
  - [53] G. B. Gelmini, S. Nussinov and M. Roncadelli, Nucl. Phys. B **209**, 157 (1982).
  - [54] K. Kainulainen, J. Maalampi and J. T. Peltoniemi, Nucl. Phys. B **358** (1991) 435.
  - [55] K. Choi and A. Santamaria, Phys. Rev. D **42**, 293 (1990); M. Kachelriess, R. Tomas and J. W. F. Valle, Phys. Rev. D **62**, 023004 (2000) [hep-ph/0001039]; R. Tomas, H. Paes and J. W. F. Valle, Phys. Rev. D **64**, 095005 (2001) [hep-ph/0103017].
  - [56] E. W. Kolb, D. L. Tubbs and D. A. Dicus, Astrophys. J. **255**, L57 (1982); G. M. Fuller, R. Mayle and J. R. Wilson, Astrophys. J. **332**, 826 (1988); Z. G. Berezhiani and A. Y. Smirnov, Phys. Lett. B **220**, 279 (1989).
  - [57] K. Enqvist, K. Kainulainen and M. J. Thomson, Nucl. Phys. B **373**, 498 (1992); X. Shi, D. N. Schramm and B. D. Fields, Phys. Rev. D **48**, 2563 (1993) [astro-ph/9307027]; N. Okada and O. Yasuda, Int. J. Mod. Phys. A **12**, 3669 (1997) [hep-ph/9606411]; S. M. Bilenky *et al.*, Astropart. Phys. **11**, 413 (1999) [hep-ph/9804421]; P. Di Bari, Phys. Rev. D **65**, 043509 (2002); Addendum-*ibid.* D **67**, 127301 (2003) [hep-ph/0108182].
  - [58] S. Hannestad, JCAP **0305**, 004 (2003) [astro-ph/0303076]; V. Barger *et al.*, Phys. Lett. B **566**, 8 (2003) [hep-ph/0305075].
  - [59] R. H. Cyburt *et al.*, Astropart. Phys. **23**, 313 (2005) [astro-ph/0408033].

- [60] R. Barbieri and A. Dolgov, Phys. Lett. B **237**, 440 (1990) and Nucl. Phys. B **349**, 743 (1991); K. Enqvist, K. Kainulainen and J. Maalampi, Phys. Lett. B **244**, 186 (1990) and *ibid.* B **249**, 531 (1990); S. Dodelson and L. M. Widrow, Phys. Rev. Lett. **72**, 17 (1994) [hep-ph/9303287].
- [61] A. D. Dolgov *et al.*, Nucl. Phys. B **548**, 385 (1999) [hep-ph/9809598].
- [62] R. Foot and R. R. Volkas, Phys. Rev. Lett. **75**, 4350 (1995) [hep-ph/9508275].
- [63] K. S. Babu and I. Z. Rothstein, Phys. Lett. B **275**, 112 (1992). L. Bento and Z. Berezhiani, Phys. Rev. D **64**, 115015 (2001) [hep-ph/0108064].
- [64] Z. Chacko *et al.*, Phys. Rev. D **70**, 085008 (2004) [hep-ph/0312267]; Z. Chacko *et al.*, Phys. Rev. Lett. **94**, 111801 (2005) [hep-ph/0405067].
- [65] J. F. Beacom, N. F. Bell and S. Dodelson, Phys. Rev. Lett. **93**, 121302 (2004) [astro-ph/0404585].
- [66] S. Hannestad, JCAP **0502**, 011 (2005) [astro-ph/0411475].